ORIGINAL RESEARCH ARTICLE

Precious Metal Distributions Between Copper Matte and Slag at High P_{SO_2} in WEEE Reprocessing

MIN CHEN, KATRI AVARMAA, LASSI KLEMETTINEN, HUGH O'BRIEN, JUNJIE SHI, PEKKA TASKINEN, DANIEL LINDBERG, and ARI JOKILAAKSO

The distributions of precious metals (gold, silver, platinum, and palladium) between copper matte and silica-saturated FeO_x-SiO_2/FeO_x-SiO_2-Al_2O_3/FeO_x-SiO_2-Al_2O_3-CaO slags were investigated at 1300 °C and P_{SO_2} = 0.5 atm. The experiments were carried out in silica crucibles under flowing CO-CO_2-SO_2-Ar gas atmosphere. The concentrations of precious metals in matte and slag were analyzed by Electron Probe X-ray Microanalysis and Laser Ablation-High-Resolution Inductively Coupled Plasma-Mass Spectrometry, respectively. The precious metal concentrations in matte and slag, as well as the distribution coefficients of precious metals between matte and slag, were displayed as a function of matte grade. The present results obtained at P_{SO_2} of 0.5 atm were compared with previous results at P_{SO_2} of 0.1 atm for revealing the effects of P_{SO_2} and selected slag modifiers (CaO and Al_2O_3) on precious metal distributions at copper matte smelting conditions. The present results also contribute experimental thermodynamic data of precious metal distributions in pyrometallurgical reprocessing of electronic waste via copper smelting processes.

https://doi.org/10.1007/s11663-021-02059-z

I. INTRODUCTION

PRECIOUS metals, including gold (Au), silver (Ag), and platinum group metals, are widely used in the electronics industry and auto-catalyst industry, due to their properties of good electrical conductivity, high melting point, and corrosion resistance.[1,2] The current higher demand for precious metals and the depletion of natural resources result in an urgent need to recover precious metals from more complicated secondary materials, especially from waste electrical and electronic equipment (WEEE),[3] in which concentrations of precious metals are significantly higher than those of natural ores.[4,5]

The most typical industrial methods for WEEE reprocessing are primary and secondary copper smelting,[6–9] followed by hydrometallurgical and electrochemical techniques. During the pyrometallurgical copper smelting processes, precious metals distribute principally between metal/matte/slag/gas phases,[10,11] and thus achieving partial recovery and purity of precious metals in the main product streams of matte and metal.[12] In order to maximize the recoveries of precious metals to the metal/matte phase, it is essential to investigate the distribution mechanism of the precious metals in the metal/matte–slag system.

Recovering precious metals from WEEE has attracted much attention worldwide in recent years. Table I summarizes the previous publications[13–31] investigating precious metals distributions in experiments simulating copper smelting conditions. A detailed summary of the available solubility/concentration and matte–slag distribution data at low P_{SO_2} of 0.1 atm[14–20] was made in our previous papers,[25–27] including the experimental techniques used and their weaknesses. To ensure the achievement of equilibrium and improve the accuracy of the experimentally measured data, a method employing high-temperature isothermal equilibration followed by rapid quenching and direct phase analysis[32,33] was developed and has been widely used for investigating

MIN CHEN, KATRI AVARMAA, LASSI KLEMETTINEN, PEKKA TASKINEN, DANIEL LINDBERG, and ARI JOKILAAKSO are with the Department of Chemical and Metallurgical Engineering, School of Chemical Engineering, Aalto University, Kemistintie 1F, P.O. Box 16100, 00076 Aalto, Finland. Contact e-mail: ari.jokilaakso@aalto.fi HUGH O'BRIEN is with the Geological Survey of Finland, Vuorimiehentie 2, 02150 Espoo, Finland. JUNJIE SHI is with the Department of Chemical and Metallurgical Engineering, School of Chemical Engineering, Aalto University and with the School of Metallurgy, Northeastern University, Shenyang 110819, China and also with the Key Laboratory for Ecological Metallurgy of Multimetallic Mineral (Ministry of Education), Northeastern University, Shenyang 110819, China.

Manuscript submitted August 24, 2020; accepted December 18, 2020.

Article published online February 25, 2021.

matte–slag equilibria.[34–44] Recently, Electron Probe X-ray Microanalysis (EPMA) and Laser Ablation-Inductively Coupled Plasma-Mass Spectrometry (LA-ICP-MS) analytical techniques were successfully applied to measure the concentrations of precious metals in matte/metal and slag,[21–31] leading to increased accuracy and reliability of the experimental data.

The distributions of precious metals have been extensively investigated between copper matte and slag at P_{SO_2} lower than 0.2 atm.[13–16,25–31] However, the use of oxygen or oxygen-enriched air as the process gas in modern copper flash smelting produces a smaller amount of off-gas with a high SO_2 concentration (> 50 vol pct).[45,46] The mechanism of matte and slag formation in flash smelting generates SO_2 with partial pressures close to 1 atm.[47] Therefore, accurate information about the distributions of precious metals between matte and slag under a high P_{SO_2} is of practical importance for thermodynamically evaluating the behaviors of precious metals in copper smelting. The primary purpose of this study was to investigate the distribution behaviors of precious metals (Au, Ag, Pt, and Pd) between copper matte and silica-saturated FeO_x-SiO_2/FeO_x-SiO_2-Al_2O_3/FeO_x-SiO_2-Al_2O_3-CaO slags at 1300 °C and P_{SO_2} of 0.5 atm, providing fundamental information for understanding and improving the recycling of precious metals from WEEE through primary copper smelting processes.

II. EXPERIMENTAL

Experiments were conducted in a similar way to our previous studies.[25,27,48,49] A high-temperature equilibration under controlled CO-CO_2-SO_2-Ar gas atmospheres followed by quenching in ice–water mixture and direct phase analyses by EPMA and LA-HR ICP-MS (HR-High Resolution) techniques was used to study the distributions of precious metals between copper matte and slag. A schematic image of the laboratory-scale furnace used is shown in Figure 1. All further details of the furnace and the gas flows used for achieving the desired atmosphere have been presented in our previous publication, which focused on the major element equilibrium in these same experiments.[49]

The slag mixtures were produced using analytical high-purity powders of Fe_2O_3 (99.998 wt pct, Alfa Aesar), SiO_2 (99.995 wt pct, Alfa Aesar), Al_2O_3 (99.99 wt pct, Sigma-Aldrich), and CaO (99.9 wt pct, Sigma-Aldrich). The copper matte mixtures were prepared by Cu_2S (99.5 wt pct) and FeS (99.9 wt pct), all from Alfa Aesar. Each metallic powder of Au (99.96 wt pct), Ag (99.95 wt pct), Pt (99.99 wt pct), and Pd (99.9 wt pct) was added into the copper matte mixture to a concentration of 1 wt pct. All precious metals were supplied by Alfa Aesar. The gas mixtures of CO (99.99 vol pct), CO_2 (99.999 vol pct), SO_2 (99.99 vol pct), and Ar (99.999 vol pct), supplied by Aga-Linde were introduced into the furnace for controlling the partial pressures of SO_2, S_2, and O_2.

All gases were regulated by DFC26 digital mass flow controllers (Aalborg, USA). The partial pressure of SO_2 was fixed at 0.5 atm in all experiments. The gas atmosphere speciations at different target matte grades were calculated by MTDATA software[50,51] using the SGTE pure substance database.[51]

In each experiment, around 0.1 g of copper matte with equal amounts of slag were pressed into a pellet and then placed into a bowl-shaped fused silica crucible. The samples were equilibrated under different CO-CO_2-SO_2-Ar gas atmospheres at experimental temperature for 4 hours.[25,48,49] The equilibrated samples were quenched into an ice–water mixture.

The quenched samples were dried, cut into half, embedded in epoxy resin (EpoFix, Struers, Denmark), and then ground and polished by metallographic methods. The polished surfaces were carbon coated using a LEICA EM SCD050 sputtering device (Leica Microsystems, Austria).

Microstructural and preliminary elemental analysis were carried out with Scanning Electron Microscope (SEM, Tescan MIRA 3, Brno, Czech Republic) equipped with an UltraDry Silicon Drift Energy Dispersive X-ray Spectrometer (EDS, Thermo Fisher Scientific, Waltham, MA, USA). The direct measurement of the concentrations of precious metals in matte, as well as the main compositions of matte and slag, were executed using a Cameca SX100 Electron Microprobe (Cameca SAS, Gennevilliers, France) coupled with five wavelength-dispersive spectrometers (WDS). The parameters were selected so that the accelerating voltage was 20 kV, beam current 60 nA, and beam diameter 100 μm and 50 to 100 μm for matte and slag, respectively. Small PGM-rich segregations (described below at the beginning of Section III) were distributed relatively evenly throughout the matte phase, and these were included in the EPMA analyses conducted with a 100-μm defocused beam. Some copper-rich veins were also found in the matte; these were avoided during the concentration quantifications.

The standards used and the X-ray lines analyzed were naturally occurring minerals quartz (Si Kα), almandine for (Al Kα), hematite (Fe Kα and O Kα), pentlandite (S Kα), diopside (Ca Kα), and synthetic pure metals Cu (Cu Kα), Au (Au Lα), Ag (Ag Lα), Pt (Pt Lα), and Pd (Pd Lα). PAP–ZAF online correction procedure was used for raw data processing.[52] Eight measuring points were taken from each phase for result averages and standard deviations.

LA-HR ICP-MS[53,54] was used to measure the precious metal concentrations in slags that were below the EPMA detection limits. The equipment and analysis procedures were exactly the same as in our previous publication dealing with the behavior of precious metals at lower sulfur dioxide partial pressure,[25] except for a slightly lower laser fluence (2.17 J/cm^2) on the sample surface. In this work, the slags of all samples were analyzed with LA-HR ICP-MS.

Fastscan mode, with a low resolution ($M/\Delta M$ = 300) for increased sensitivity, was applied for collecting the time-resolved analysis (TRA) signals. Signal processing was performed using the Glitter software.[55] The

Table I. A Summary of the Literature on Precious Metals Distributions in Copper Smelting

Equilibrium System	Slag System	P_{SO_2}/atm	LogP_{O_2}/atm	Temperature/°C	Precious Metals	Crucible	Analytical Methods	Ref.
MgO-Saturated Slag								
Cu Matte–Slag	FeO_x-SiO_2	Not specified	− 11.5	1250	Ag	magnesia	ICP-AES	13
Metallic Pt-Slag	FeO_x-SiO_2	—	− 8 to − 6	1300	Pt	magnesia	ICP and ICP-MS	14
Pt-Cu Alloy-Slag	FeO_x-SiO_2	—	− 9 to − 6	1300	Pt	magnesia	ICP and ICP-MS	14
Metallic Pd-Slag	FeO_x-SiO_2	—	− 9 to − 6	1300	Pd	magnesia	ICP and ICP-MS	15
Pd-Cu Alloy-Slag	FeO_x-SiO_2	—	− 9 to − 7	1300	Pd	magnesia	ICP and ICP-MS	15
Cu Matte–Slag	FeO_x-SiO_2	0.1	− 9 to − 7	1300	Au, Pt, Pd	magnesia	ICP and ICP-MS	14–16
Cu Matte–Slag	FeO_x-CaO-(SiO_2, MgO) FeO_x-SiO_2-MgO	0.1 to 1	− 7 to − 3	1250 to 1300	Ag	magnesia	ICP*	17–20
SiO_2-Saturated Slag								
Cu Alloy-Slag	FeO_x-SiO_2-(Al_2O_3-CaO)	—	− 7 to − 5	1300	Ag, Au, Pt, Pd	silica	EPMA and LA-ICP-MS	21
Cu Alloy-Slag	FeO_x-SiO_2	—	− 8 to − 4	1250 to 1350	Ag, Au, Pt, Pd	silica	EPMA and LA-ICP-MS	22
Cu Alloy-Slag	FeO_x-SiO_2-Al_2O_3(-CaO)	—	− 10 to − 5	1300	Ag	silica	EPMA	23
Cu alloy-Slag	FeO_x-SiO_2	—	− 10 to − 5	1250 to 1300	Ag	silica	EPMA and LA-ICP-MS	24
Cu Matte–Slag	FeO_x-SiO_2-(Al_2O_3-CaO)	0.1	− 8 to − 7	1250 to 1350	Au, Ag, Pt, Pd	silica	EPMA and LA-ICP-MS	25–27
Cu Matte–Slag	FeO_x-SiO_2	0.25	− 9 to − 8	1200	Au, Ag	silica	EPMA and LA-ICP-MS	28
Metallic Au-Slag	FeO_x-SiO_2	—	− 8 to − 6.5	1250 to 1300	Au, Ag	silica	EPMA and LA-ICP-MS	28
Spinel-Saturated Slag								
Cu alloy-Slag	FeO_x-SiO_2-Al_2O_3	—	− 10 to − 6	1300	Au, Ag	alumina	EPMA and LA-ICP-MS	29
Cu alloy-Slag	FeO_x-SiO_2-Al_2O_3(-CaO)	—	− 10 to − 5	1300	Au, Ag, Pt, Pd	alumina	EPMA and LA-ICP-MS	30
Cu Matte–Slag	FeO_x-SiO_2	0.25	− 9 to − 8	1200	Au, Ag	Fe_3O_4	EPMA and LA-ICP-MS	31

ICP, inductively coupled plasma; *, no further details of the analysis technique given; ICP-AES, inductively coupled plasma atomic emission spectrometry; ICP-MS, inductively coupled plasma atomic mass spectrometry; LA, laser ablation allowing direct microsampling by laser beam rather than requiring (imperfect) bulk sample separation.

concentrations of precious metals in slags measured by LA-HR ICP-MS were calculated using isotopes of ^{197}Au for gold, ^{104}Pd for palladium, an average of ^{107}Ag and ^{109}Ag for silver, and an average of ^{194}Pt, ^{195}Pt, and ^{196}Pt for platinum. Table II shows the elemental detection limits for EPMA and LA-HR ICP-MS.

The TRA signals in different samples showed either completely homogeneous dissolution of the precious metals into the slag, or the presence of some nano-/micronuggets containing higher precious metal concentrations.[56] Examples of both cases are shown in Figure 2. The occurrence of the nuggets in the slags did not follow any particular pattern: they were observed in some samples with and without Al_2O_3 and CaO. In most cases, it was possible to select inclusion-free segments of the signal profiles for quantitative concentration calculations, as marked in Figure 2(b) with the light gray color.

III. RESULTS AND DISCUSSION

Typical microstructures of the copper matte equilibrated with different silica-saturated slags for target matte grade of 60 wt pct Cu are shown in Figure 3. The glassy slag phase was homogeneous; however, copper-rich veins and small segregations with higher precious metal concentrations were distributed randomly in the matte phase, most likely due to an insufficient quenching rate, as seen earlier.[25,48,49] The concentrations of precious metals in matte and slag with standard deviations ($\pm$ 1σ) are listed in Table III. The results for the major elements can be seen in our previous study.[49]

A. *Concentrations of Precious Metals in Matte*

The concentrations of precious metals in matte with standard deviations, measured by EPMA, are displayed as a function of matte grade in Figure 4. The results obtained at 1300 °C and P_{SO_2} of 0.1 atm from our previous study,[25] shown as open symbols, are also plotted in the graphs for comparison with the results of few other studies.[27,28] The concentrations of all precious metals in matte, equilibrated with different slags, kept almost constant over the entire matte grade range studied, suggesting that the deportment of precious metals into the matte phase was not affected by slag modifiers. The results for silver and palladium obtained at P_{SO_2} of 0.5 atm are within error of the previous data achieved at P_{SO_2} of 0.1 atm[25] at the same matte grade. This indicates that the deportment of silver and palladium into the matte phase was not affected by the prevailing P_{SO_2}. However, the results for gold and platinum obtained at P_{SO_2} of 0.5 atm are approximately 0.1 and 0.2 wt pct higher than the previous results at 0.1 atm P_{SO_2}, respectively. The present results fit well with the observations by Avarmaa *et al.*[27] but are on the higher side of the results by Shishin *et al.*[28] Avarmaa *et al.*[27] reported that the silver concentration in matte was sensitive to the temperature and it decreased with increasing temperature. The higher volatility of silver at higher temperatures was regarded as the main factor for the decreasing concentration trend.[22,27]

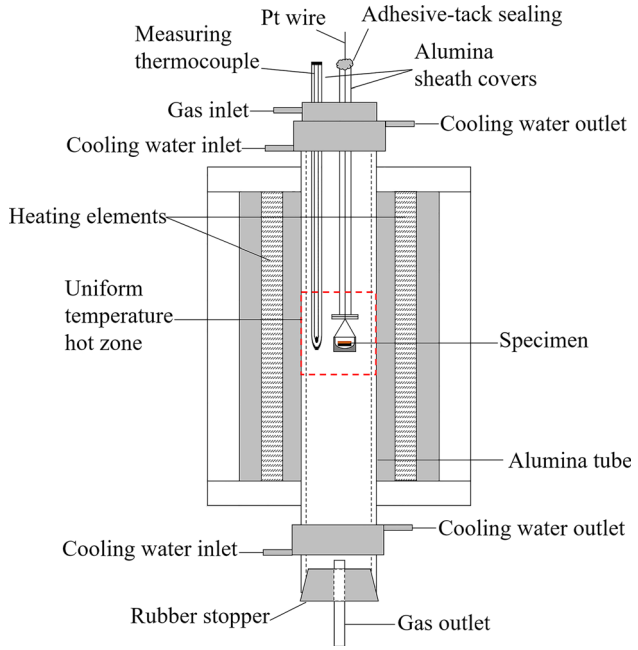

Fig. 1—Schematic diagram of the vertical furnace for the equilibration experiments.

B. *Concentrations of Precious Metals in Slags*

During recycling of WEEE through copper smelting routes, it is essential to minimize the losses of precious metals in the slag. Precious metal concentration data are helpful in analyzing and controlling these losses. The concentrations of precious metals in slags with standard deviations, measured by LA-HR ICP-MS, were plotted in Figure 5 against the matte grade.

Figure 5(a) indicates that the concentrations of gold dissolved in all silica-saturated slags in equilibrium with copper matte were typically between 0.4 and 10 ppmw, and they decreased with increasing matte grade (*i.e.,* with increasing oxygen partial pressure), as reported by Avarmaa *et al.*[26] and Shishin *et al.*[28] However, an opposite, increasing trend for gold solubility in sulfur-free iron silicate slag equilibrated with Au-Pd alloy was observed by Borisov and Palme,[57] reporting that the gold solubility increased from 1 to approximately 10 ppm with increasing oxygen partial pressure from 10^{-8} to 10^{-3} atm. Shishin *et al.*[28] measured the gold solubility in FeO_x-SiO_2 slag in equilibrium with metallic gold at 1250 °C to 1300 °C. The values reported were lower than 4 ppmw,[28] which appears to be somewhat lower than the ones obtained in this study. The present results for gold in slags obtained at P_{SO_2} of 0.5 atm were almost identical to the observations at P_{SO_2} = 0.1 atm, suggesting that gold concentration in the slag was not

Table II. The Detection Limits of EPMA and LA-HR ICP-MS for Elements Investigated in Matte and Slag (ppmw)

Element/Phase		O	Si	Al	S	Ca	Fe	Cu	Pd	Ag	Pt	Au
EPMA Detection Limits	Matte	1270	250	250	140	110	200	370	170	170	490	660
	Slag	1000	210	190	110	90	200	270	140	140	390	540
		^{29}Si	^{197}Au	^{107}Ag	^{109}Ag	^{194}Pt	^{195}Pt	^{196}Pt	^{104}Pd			
LA-HR ICP-MS Detection Limits	Slag	4.5000	0.0009	0.0030	0.0030	0.0017	0.0017	0.0024	0.0260			

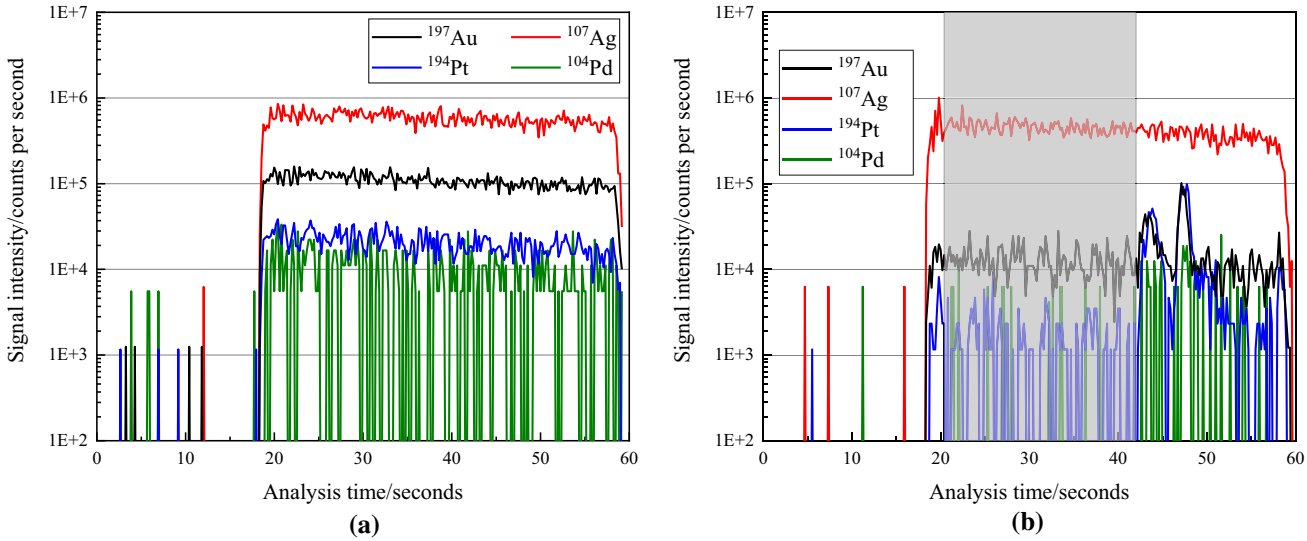

Fig. 2—Examples of TRA signals in two different samples. (*a*) sample code 5; (*b*) sample code 23. When nano-/micronuggets were observed in the signals, only the areas free of these nuggets, such as the area marked with light gray color in (*b*), were used to calculate quantitative concentrations. For the interpretation of the sample codes, please refer to Table III.

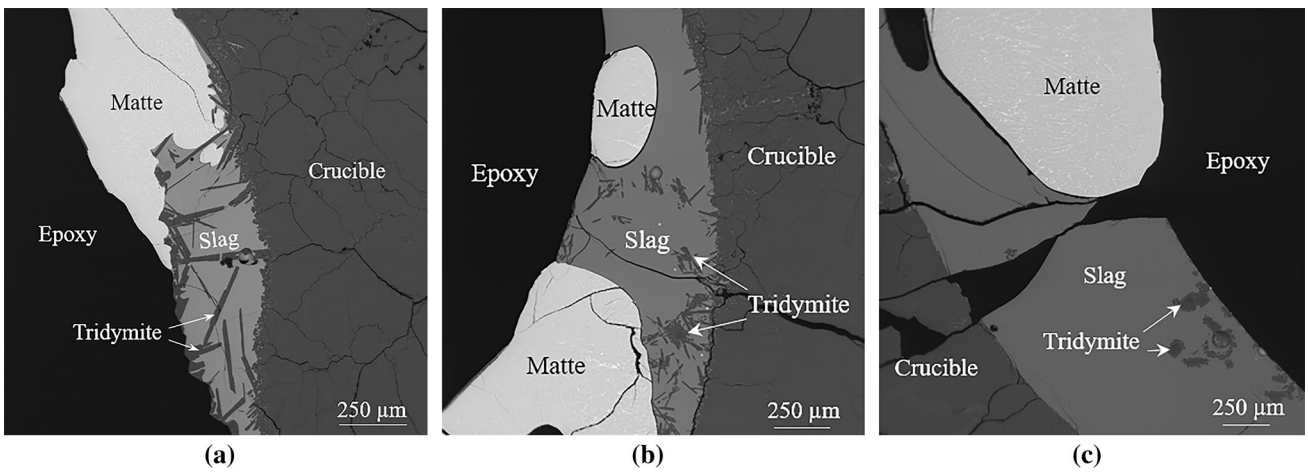

Fig. 3—Typical microstructures of the matte phase in equilibrium with slag and tridymite under P_{SO_2} of 0.5 atm and 1300 °C (*a*) matte (57.1 wt pct Cu) with FeO_x-SiO_2 slag; (*b*) matte (61.1 wt pct Cu) FeO_x-SiO_2-Al_2O_3 slag; (*c*) matte (63.8 wt pct Cu) FeO_x-SiO_2-Al_2O_3-CaO slag.

sensitive to the prevailing SO_2 partial pressure. Gold losses in silica-saturated slags were, however, significantly suppressed by the addition of alumina and lime independent of P_{SO_2}.

Toguri and Santander[58] investigated the distribution of gold between copper-gold alloy and silica-saturated FeO_x-SiO_2 slag at 1250 °C to 1350 °C and P_{SO_2} of 10^{-10} to 10^{-7} atm. The gold concentration in slag was

Table III. Measured Concentrations of Copper and Precious Metals in Matte and Slag at 1300 °C and P_{SO_2} of 0.5 atm

Type of Slag	Code	$Log_{10}P_{O_2}$/ atm	*Average Concentration in Matte ± Standard Deviation (Wt pct)					**Average Concentration in Slag ± Standard Deviation (ppmw)			
			Cu	Au	Ag	Pt	Pd	Au	Ag	Pt	Pd
FeO_x-SiO_2	1	− 7.09	73.73 ± 0.36	0.57 ± 0.07	1.14 ± 0.16	0.62 ± 0.15	0.81 ± 0.08	1.24 ± 0.41	75.99 ± 14.24	0.74 ± 0.08	1.76 ± 0.25
	2	− 7.09	73.71 ± 0.37	0.55 ± 0.10	0.96 ± 0.15	0.54 ± 0.20	0.79 ± 0.08	1.29 ± 0.39	74.34 ± 14.63	0.66 ± 0.16	1.39 ± 0.35
	3	− 7.36	66.65 ± 0.18	0.77 ± 0.07	1.02 ± 0.06	0.80 ± 0.15	0.95 ± 0.06	3.25 ± 0.86	48.00 ± 14.44	2.99 ± 0.44	4.13 ± 0.50
	4	− 7.36	66.57 ± 0.12	0.84 ± 0.06	1.01 ± 0.05	1.10 ± 0.05	0.95 ± 0.06	4.95 ± 1.15	66.35 ± 16.61	4.19 ± 0.94	5.91 ± 1.50
	5	− 7.42	63.54 ± 0.29	0.68 ± 0.11	0.96 ± 0.09	0.66 ± 0.20	0.84 ± 0.11	7.79 ± 1.68	74.55 ± 17.75	3.25 ± 0.62	4.88 ± 0.75
	6	− 7.42	63.39 ± 0.34	0.77 ± 0.06	0.93 ± 0.08	0.86 ± 0.13	0.90 ± 0.06	6.50 ± 1.03	69.98 ± 11.79	3.62 ± 0.78	4.83 ± 1.06
	7	− 7.56	57.97 ± 0.37	0.68 ± 0.10	0.92 ± 0.05	0.82 ± 0.08	0.79 ± 0.07	10.31 ± 3.24	68.75 ± 21.59	4.32 ± 0.78	5.76 ± 1.28
	8	− 7.56	57.10 ± 0.47	0.56 ± 0.07	0.81 ± 0.08	0.74 ± 0.08	0.72 ± 0.08	9.48 ± 3.05	57.18 ± 18.60	5.74 ± 1.03	10.59 ± 3.00
FeO_x-SiO_2-Al_2O_3	9	− 7.09	74.25 ± 0.26	0.72 ± 0.12	1.15 ± 0.03	0.83 ± 0.21	0.95 ± 0.10	0.65 ± 0.13	93.50 ± 12.38	0.16 ± 0.04	0.76 ± 0.31
	10	− 7.09	73.74 ± 0.40	0.74 ± 0.09	1.10 ± 0.06	0.87 ± 0.10	0.96 ± 0.10	0.85 ± 0.08	99.36 ± 23.86	0.20 ± 0.04	0.76 ± 0.30
	11	− 7.36	68.60 ± 0.11	0.86 ± 0.03	1.06 ± 0.05	0.84 ± 0.12	1.03 ± 0.03	1.48 ± 0.37	59.94 ± 8.80	0.63 ± 0.12	1.25 ± 0.46
	12	− 7.36	68.17 ± 0.23	0.77 ± 0.10	0.92 ± 0.13	0.98 ± 0.09	0.86 ± 0.11	1.83 ± 0.17	78.10 ± 11.10	0.60 ± 0.14	0.97 ± 0.24
	13	− 7.42	65.62 ± 0.20	0.78 ± 0.07	0.92 ± 0.08	0.93 ± 0.11	0.87 ± 0.09	2.21 ± 0.26	63.78 ± 7.45	0.60 ± 0.05	1.25 ± 0.27
	14	− 7.42	66.38 ± 0.14	0.77 ± 0.04	0.96 ± 0.08	0.94 ± 0.05	0.88 ± 0.08	1.93 ± 0.16	79.32 ± 8.01	0.71 ± 0.09	1.00 ± 0.18
	15	− 7.56	61.06 ± 0.30	0.74 ± 0.06	0.87 ± 0.14	0.89 ± 0.04	0.85 ± 0.07	2.88 ± 0.30	63.35 ± 10.19	0.58 ± 0.05	1.05 ± 0.38
	16	− 7.56	61.84 ± 0.23	0.73 ± 0.10	0.81 ± 0.07	0.85 ± 0.10	0.86 ± 0.09	2.65 ± 0.24	66.45 ± 9.38	0.68 ± 0.17	1.20 ± 0.26
FeO_x-SiO_2-Al_2O_3-CaO	17	− 7.09	74.05 ± 0.39	0.65 ± 0.10	1.23 ± 0.10	0.78 ± 0.17	0.92 ± 0.16	0.39 ± 0.09	73.73 ± 14.31	0.20 ± 0.08	0.48 ± 0.16
	18	− 7.09	73.88 ± 0.39	0.71 ± 0.15	1.40 ± 0.05	0.84 ± 0.19	0.91 ± 0.15	0.54 ± 0.09	85.11 ± 7.31	0.94 ± 0.19	0.43 ± 0.17
	19	− 7.36	70.02 ± 0.37	0.81 ± 0.13	1.03 ± 0.19	0.97 ± 0.15	0.95 ± 0.15	0.63 ± 0.05	53.11 ± 9.54	0.16 ± 0.03	0.36 ± 0.18
	20	− 7.36	70.19 ± 0.20	0.87 ± 0.08	1.00 ± 0.06	1.02 ± 0.07	0.97 ± 0.07	0.81 ± 0.09	54.67 ± 8.59	0.21 ± 0.09	0.36 ± 0.20
	21	− 7.42	68.02 ± 0.13	0.74 ± 0.06	0.95 ± 0.07	0.97 ± 0.09	0.90 ± 0.06	0.81 ± 0.06	48.73 ± 7.17	0.19 ± 0.09	0.39 ± 0.18
	22	− 7.42	67.73 ± 0.18	0.70 ± 0.07	0.90 ± 0.09	0.96 ± 0.13	0.86 ± 0.06	0.70 ± 0.10	51.84 ± 10.51	0.24 ± 0.10	0.30 ± 0.13
	23	− 7.56	64.42 ± 0.28	0.65 ± 0.08	0.86 ± 0.09	0.76 ± 0.09	0.78 ± 0.09	1.06 ± 0.07	47.70 ± 4.99	0.28 ± 0.18	0.39 ± 0.07
	24	− 7.56	63.80 ± 0.58	0.85 ± 0.21	1.13 ± 0.29	0.93 ± 0.15	1.01 ± 0.25	0.91 ± 0.08	46.17 ± 4.55	0.22 ± 0.09	0.32 ± 0.17

*EPMA measurement.
**LA-HR ICP-MS measurement.

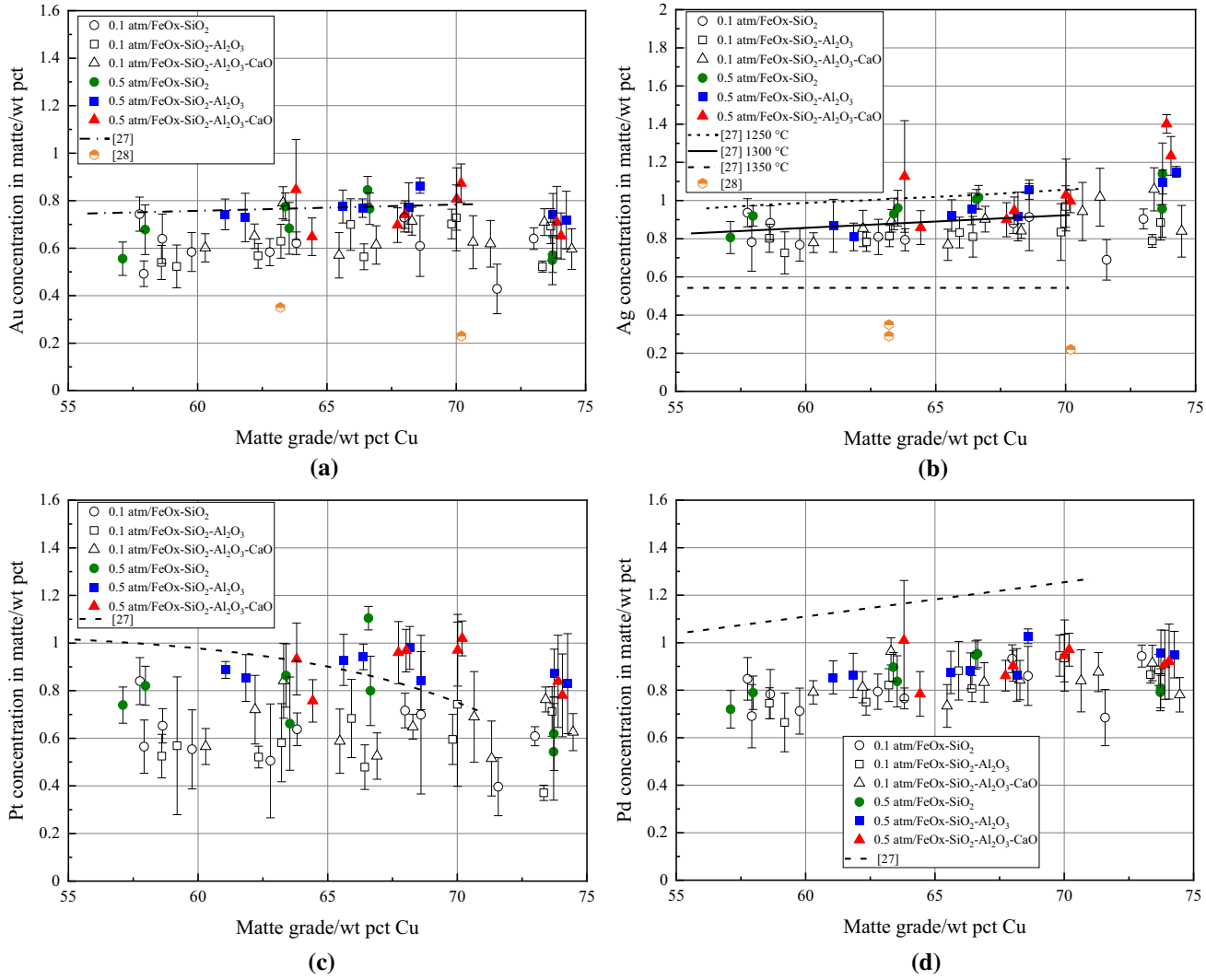

Fig. 4—Precious metals concentrations in matte at 1300 °C and P_{SO_2} = 0.5 atm; (*a*) gold; (*b*) silver; (*c*) platinum; (*d*) palladium; colored symbols—present study; open symbols—our previous study[25]

reported to be several hundreds of ppm,[58] which is significantly higher than the present results. In the study by Avarmaa *et al.*,[21,29] a remarkably lower gold solubility (< 0.2 ppmw) was observed in alumina/silica-saturated FeO_x-SiO_2-Al_2O_3 slags in a sulfur-free system. Choi and Cho[59] measured the gold concentrations in silica-saturated FeO_x-SiO_2 slags equilibrated with nickel-copper matte at 1300 °C, and they reported that the concentrations of gold in these slags were approximately 100 to 800 ppmw, which are similar to the results by Toguri and Santander.[58] The impact of Al_2O_3, MgO, and CaO on decreasing the gold concentrations in slags were also observed in their study.[59] Altman and Kellogg[60] measured a concentration of gold in silica-saturated FeO_x-SiO_2 slag at 1224 °C to 1286 °C of approximately 80 ppmw. Taylor and Jeffes[61] reported that the gold concentration in iron silicate slags at 1300 °C to 1450 °C and P_{O_2} 10^{-13} to 10^{-5} atm was around 40 to 80 ppmw. In previous studies,[58–61] the concentrations of gold in slags were analyzed following physical separation of copper-gold alloy and slag. An incomplete separation of copper-gold alloy and slag most likely contributed to the higher gold concentration in slags in those studies.[58–61]

Compared with the other three precious metals, silver exhibited a significantly higher concentration in silica-saturated iron silicate slags, varying between approximately 50 and 100 ppmw, as shown in Figure 5(b), which are on the higher side of the observations by Shishin *et al.*[28] The silver concentration in FeO_x-SiO_2 slag in the present study was kept almost constant over the entire matte grade range investigated, fluctuating around 60 ppmw, similar to the results by Louey *et al.*[13] However, increasing trends were found for alumina-containing and alumina + lime-containing slags. A similar increasing trend was also reported by Avarmaa *et al.*[29] and Hidayat *et al.*[24] for alumina-saturated FeO_x-SiO_2-Al_2O_3 slag and silica-saturated FeO_x-SiO_2 slag in equilibrium with metallic copper at 1300 °C, respectively. Avarmaa *et al.*[26] also reported that the concentration of silver in silica-saturated FeO_x-SiO_2 slags, equilibrated with copper matte, was dependent on

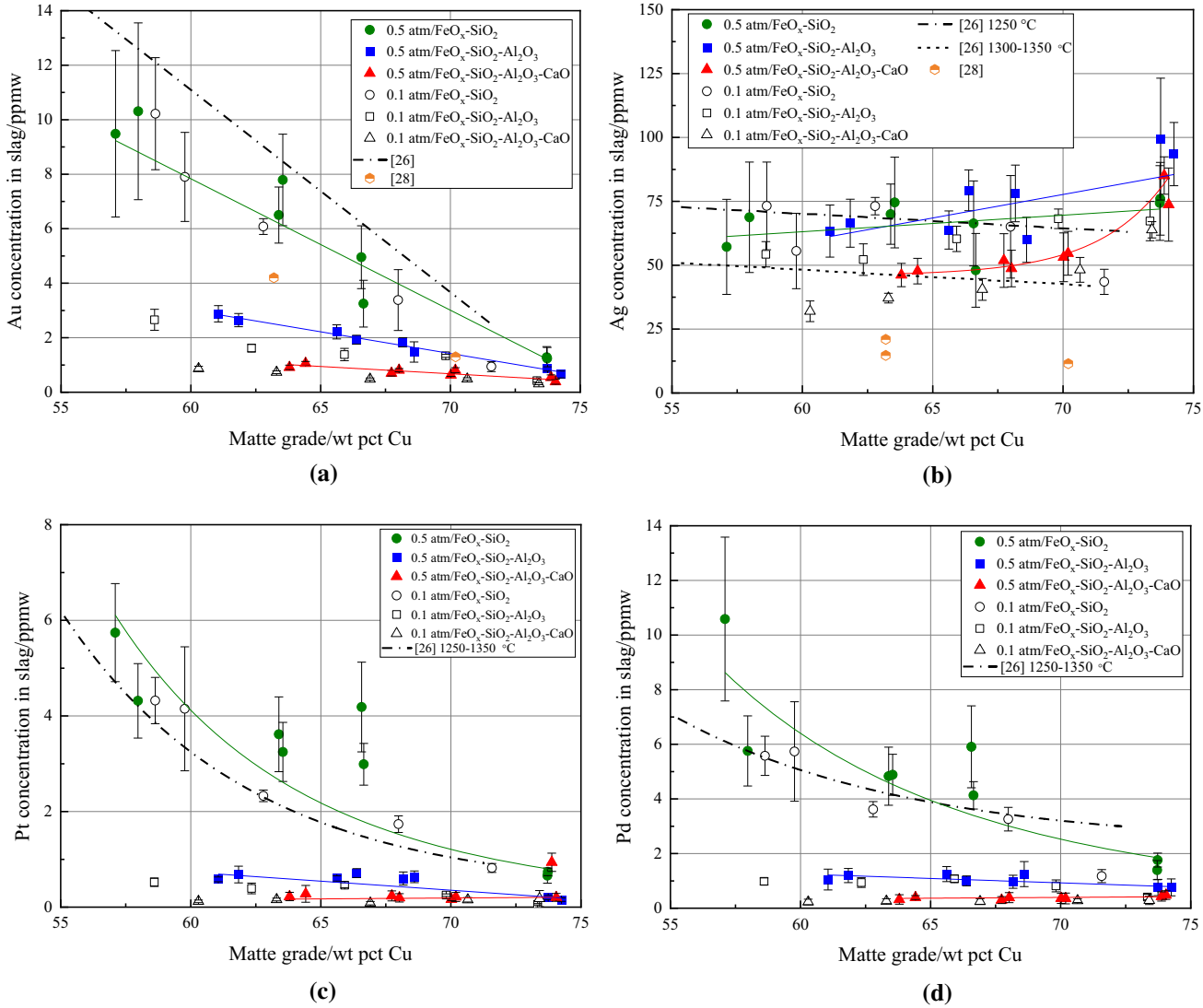

Fig. 5—Precious metals concentrations in silica-saturated iron silicate slags at 1300 °C and P_{SO_2} of 0.5 atm; (*a*) gold; (*b*) silver; (*c*) platinum; (*d*) palladium; colored symbols—present study; open symbols—our previous study[25]

temperature and it decreased with increasing temperature. Shishin *et al.*[62] investigated the behavior of silver between metallic lead and silica-saturated FeO_x-SiO_2 slag at 1000 °C to 1200 °C, and the silver concentration in the slag was reported to be approximately 45 to 47 ppmw, which was slightly lower than the present results for FeO_x-SiO_2 slags in equilibrium with copper matte. The silver concentrations in slags obtained at 0.1 and 0.5 atm P_{SO_2} seemed not to be affected by the P_{SO_2}, similar to the results for gold, platinum, and palladium. The independence of silver concentrations in slags to P_{SO_2} was also reported by Roghani *et al.*[17–20] for magnesia-saturated FeO_x-CaO/FeO_x-SiO_2-CaO/FeO_x-SiO_2-MgO/FeO_x-SiO_2-MgO-CaO slags at P_{SO_2} of 0.1, 0.5, and 1 atm. The use of magnesia crucibles in previous studies[14–20] resulted in MgO dissolution into the slags. The concentrations of precious metals were analyzed by wet chemical analysis techniques after physically separating the matte and slag, which may have caused erroneous results due to incomplete phase separation. The factors mentioned above lead to significant gaps and discrepancies between the present observations and the reported results by Roghani *et al.*[17–20]

The concentrations of platinum and palladium in FeO_x-SiO_2 and FeO_x-SiO_2-Al_2O_3 slags have similar decreasing trends with increasing matte grade (*i.e.*, increasing oxygen partial pressure), as reported by Avarmaa *et al.*[26] In the study by Yamaguchi[14,15] and Baba *et al.*,[63] the concentrations of platinum and palladium in FeO_x-SiO_2 slags, equilibrated with pure metallic platinum/palladium, increased from 3 to 7 ppmw and 7 to 20 ppmw, respectively, with increasing oxygen partial pressure from 10^{-9} to 10^{-6} atm at 1300 °C. Those results are opposite to the present decreasing trends but agree well with the observation by Shuva *et al.*[64] Klemettinen *et al.*[65] reported that the platinum solubility in alumina spinel-saturated FeO_x-SiO_2-Al_2O_3 slag equilibrated with pure platinum increased from around 15 to 80 ppbw when the P_{O_2} increased from 10^{-10} to 10^{-5} atm. The solubility data reported by

Klemettinen *et al.*[65] were extremely low, even at the highest P_{O_2} of copper-making conditions, around 10^{-5} atm. Murata and Yamaguchi[66] investigated the recovery of platinum and palladium from an Al_2O_3-CaO-SiO_2 slag using Cu or Cu_2O. The concentrations of platinum in the slag were around 80 and 2 ppmw after being equilibrated with metallic Cu and Cu_2O at 1450 °C for 12 hours, respectively. Simultaneously, the results for palladium were reported to be 130 and 1.3 ppmw, respectively. The addition of alumina and lime decreased the platinum and palladium losses in iron silicate slags significantly in the present study, even down to 0.5 ppmw. Similarly, Wiraseranee *et al.*[67] reported that the solubility of platinum in Na_2O-SiO_2-based slags decreased with increasing contents of alumina, magnesia, ferric oxide, and copper oxide in the slags.

C. *Distributions of Precious Metals Between Matte and Slag*

The distribution coefficients of precious metals between copper matte and slag, $L^{m/s}(Me)$, were calculated based on Eq. [1]:

$$\mathrm{Log}_{10}\left[L^{m/s}(Me)\right] = \mathrm{Log}_{10}\left([\text{wt pct Me}]_{\text{inmatte}}/(\text{wt pct Me})_{\text{inslag}}\right), \quad [1]$$

where [wt pct Me] and (wt pct Me) refer to the average concentrations of precious metals in matte and slag, respectively. The obtained distribution coefficients for gold, silver, platinum, and palladium are displayed as a function of matte grade in Figure 6 together with selected literature data.

All precious metals were preferentially concentrated in the matte and their distributions were affected by the matte grade. Figure 6(a) indicates that the deportment of gold into the matte phase equilibrated with all slags were favored by increasing matte grade, which agrees well with the observations in our previous study at P_{SO_2} 0.1 atm[25] and by Avarmaa *et al.*[26] The addition of alumina and lime increased the logarithmic distribution coefficient of gold by approximately 0.4 and 0.8, respectively, at the matte grade of 65 wt pct Cu. Similar positive effects of alumina and lime on increasing the deportment into the matte phase were also observed for platinum and palladium, however, the increasing $L^{m/s}$ trends as a function of matte grade were less obvious for the alumina + lime-containing slag. Chen *et al.*[68] determined the distribution coefficient of gold between metallic copper and silica-saturated FeO_x-SiO_2 slag in the slag/matte/metal equilibrium system, reporting that the logarithmic value decreased with increasing the matte grade from 65 to 80 wt pct Cu, which is opposite to the tendency observed in the present study. Importantly, the distribution coefficients of the precious metals investigated seemed unaffected by the prevailing P_{SO_2}. Therefore, from the point of view of thermodynamics it can be concluded that the use of oxygen or oxygen-enriched air as the blowing gas should have no impact on the recovery of these precious metals in industrial copper flash smelting processes.

Figure 6(b) shows that the distribution coefficient of silver between copper matte and FeO_x-SiO_2 slag stayed almost constant over the entire matte grade range studied, close to that reported by Avarmaa *et al.*[26] However, opposite downward trends with increasing matte grade were observed for the matte/FeO_x-SiO_2-Al_2O_3 and matte/FeO_x-SiO_2-Al_2O_3-CaO systems. The trend line of the distribution coefficients of silver between matte and FeO_x-SiO_2 slag is on the higher side of that between matte and FeO_x-SiO_2-Al_2O_3 slag but on the lower side of that between matte and FeO_x-SiO_2-Al_2O_3-CaO slag. Thus, the deportment of silver into the matte phase may be improved by lime addition, whereas alumina had no significant impact when compared with the results for FeO_x-SiO_2 slag. Similar effects of alumina and lime on the deportment of silver into the metallic copper were also reported by Avarmaa.[69] The distribution coefficient of silver between matte and FeO_x-SiO_2-MgO slag reported by Roghani *et al.*[20] was slightly higher than the present results between matte and FeO_x-SiO_2-Al_2O_3 slag. The $L^{m/s}$Ag between matte and FeO_x-SiO_2-MgO-CaO slag obtained by Roghani *et al.*[19] was significantly higher than the present results between matte and FeO_x-SiO_2-Al_2O_3-CaO slag, indicating that magnesia has a larger impact than alumina on improving the recovery of silver into the matte phase. Kashima *et al.*[70] obtained distribution coefficients of silver between white metal and silica-saturated iron silicate slag at 1300 °C and P_{SO_2} of 0.0007 to 0.20 atm. Similar to the results in this study the $L^{m/s}$ Ag were found to be independent of the P_{SO_2}.[17–20]

The distribution coefficients of platinum and palladium between matte and FeO_x-SiO_2/FeO_x-SiO_2-Al_2O_3 slag had similar increasing trends with increasing matte grade,[26] but the slope for platinum was steeper. Alumina addition improved the logarithmic distribution coefficients of platinum and palladium by approximately 0.7 and 0.6, respectively, at a matte grade of 65 wt pct Cu. However, the $\mathrm{Log}_{10}[L^{m/s}Pt]$ and $\mathrm{Log}_{10}[L^{m/s}Pd]$ for the matte/FeO_x-SiO_2-Al_2O_3-CaO slag system kept almost constant at 4.6 and 4.4, respectively. Yamaguchi[14,15] and Henao *et al.*[16] reported that the logarithmic distribution coefficients of platinum and palladium remained constant at around 3 in the matte grade range of 40 to 65 wt pct Cu, after which it started to decrease at higher matte grades. The incomplete phase separation of matte and slag may have led to the lower distribution coefficients in those studies.[14–16]

IV. CONCLUSIONS

The distribution equilibria of gold, silver, platinum, and palladium between copper mattes and silica-saturated FeO_x-SiO_2/FeO_x-SiO_2-Al_2O_3/FeO_x-SiO_2-Al_2O_3-CaO slags were determined at 1300 °C and at a

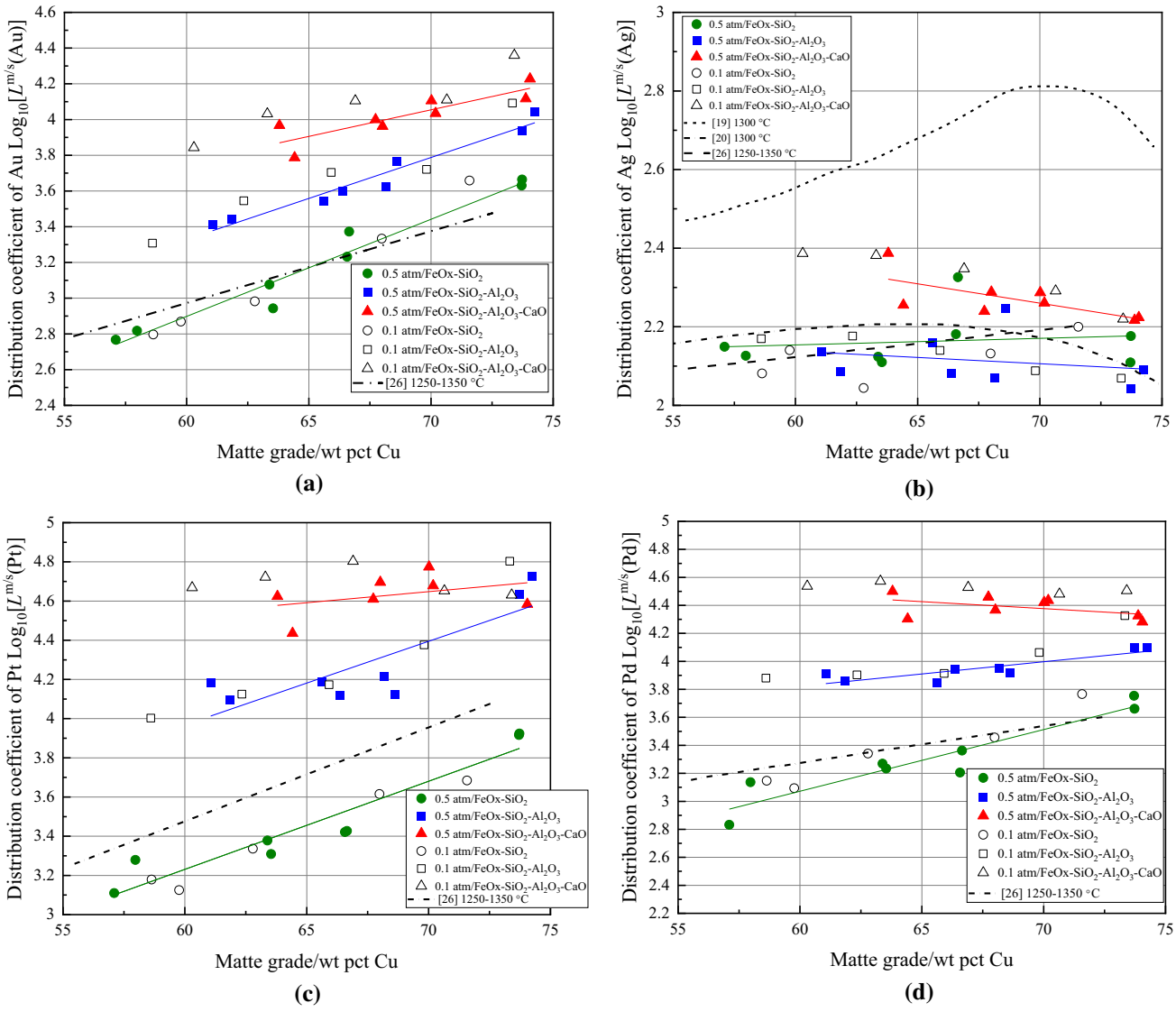

Fig. 6—Logarithmic distribution coefficients of precious metals between copper matte and silica-saturated iron silicate slags as a function of matte grade at 1300 °C and P_{SO_2} of 0.5 atm: (*a*) gold; (*b*) silver; (*c*) platinum; (*d*) palladium; colored symbols—present study; open symbols—our previous study[25]

high P_{SO_2} of 0.5 atm using a high-temperature equilibration/quenching/EPMA/LA-HR ICP-MS technique. The present results help to deepen our understanding of the behaviors of precious metals in the copper flash smelting processes at high P_{SO_2} conditions.

A comparison of the results obtained at P_{SO_2} of 0.1 and 0.5 atm shows that the concentrations of silver and palladium in matte at a fixed matte grade were not affected by the prevailing P_{SO_2}, however, the gold and platinum concentrations in matte were somewhat increased with higher P_{SO_2}. The precious metal concentrations in the slags were independent of P_{SO_2}. The concentrations of gold, platinum, and palladium in slags can be effectively decreased by alumina and lime additions, and by increasing the matte grade.

All the precious metals were found to highly distribute into the matte phase. Higher matte grades and addition of alumina and lime were proven to have positive effects on increasing the $L^{m/s}$(Au), $L^{m/s}$(Pt), and $L^{m/s}$(Pd) and thus their recoveries to the sulfide matte. Consequently, it is essential to carefully control the slag composition and matte grade during the pyro-reprocessing of precious metals containing waste materials with the purpose of maximizing the recoveries of precious metals.

ACKNOWLEDGMENTS

This work was partly financially supported by the Aalto University School of Chemical Engineering and

the Business Finland financed SYMMET Project [Grant #3891/31/2018] and utilized the Academy of Finland's RawMatTERS Finland Infrastructure (RAMI) based at Aalto University, GTK Espoo and VTT Espoo. The contribution of Mr. Lassi Pakkanen of Geological Survey of Finland (GTK) is specially appreciated for conducting the EPMA analyses. Min Chen acknowledges the China Scholarship Council (CSC) [Grant #201806370217] for supporting his study at Aalto University. Lassi Klemettinen is grateful for the Finnish Steel and Metal Producers' Fund for a doctoral project grant.

CONFLICT OF INTEREST

All authors declare that they have no conflict of interest.

FUNDING

Open access funding provided by Aalto University.

OPEN ACCESS

REFERENCES

1. M.L. Zientek and P.J. Loferski: *US Geological Survey Fact Sheet*, 2014, p. 3064. https://dx.doi.org/10.3133/fs20143064.
2. S. Zhang, Y. Ding, B. Liu, and C.C. Chang: *Waste Manag.*, 2017, vol. 65, pp. 113–27. https://doi.org/10.1016/j.wasman.2017.04.003.
3. R.G. Charles, P. Douglas, I.L. Hallin, I. Matthews, and G. Liversage: *Waste Manag.*, 2017, vol. 60, pp. 505–20. https://doi.org/10.1016/j.wasman.2016.11.018.
4. A. Tuncuk, V. Stazi, A. Akcil, E.Y. Yazici, and H. Deveci: *Miner. Eng.*, 2012, vol. 25 (1), pp. 28–37. https://doi.org/10.1016/j.mineng.2011.09.019.
5. A. Cesaro, A. Marra, K. Kuchta, V. Belgiorno, and E.D. Van Hullebusch: *Glob. NEST J.*, 2018, vol. 20, pp. 743–50. https://doi.org/10.30955/gnj.002623.
6. J. Brusselaers, F.E. Mark, and L. Tange: *PlasticsEurope, Brüssel*, 2006, Belgium. http://www.plasticseurope.org/.
7. C. Hagelüken: *Acta Metall. Slovaca*, 2006, vol. 12, pp. 111–20.
8. C. Hagelüken: *World Metall.-Erzmet.*, 2006, vol. 59 (3), pp. 152–61.
9. A. Lennartsson, F. Engström, C. Samuelsson, B. Björkman, and J. Pettersson: *J. Sustain. Metall.*, 2018, vol. 4 (2), pp. 222–32. https://doi.org/10.1007/s40831-018-0157-5.
10. M.A.H. Shuva, M.A. Rhamdhani, G.A. Brooks, S. Masood, and M.A. Reuter: *J. Clean. Prod.*, 2016, vol. 131, pp. 795–809. https://doi.org/10.1007/s40831-018-0157-5.
11. E. Jak, T. Hidayat, V. Prostakova, D. Shishin, M. Shevchenko, and P.C. Hayes: *Proceedings of EMC*, 2019, pp. 587–604.
12. F. Tesfaye, D. Lindberg, J. Hamuyuni, P. Taskinen, and L. Hupa: *Miner. Eng.*, 2017, vol. 111, pp. 209–21. https://doi.org/10.1016/j.mineng.2017.06.018.
13. R. Louey, D.R. Swinbourne, and T. Lehner: *Proceedings of AusIMM*. The Australian Institute of Mining and Metallurgy, 1999, pp. 31–36.
14. K. Yamaguchi: *Proceedings of Copper 2010*, GDMB, Clausthal-Zellerfeld, Germany, 2010, pp. 1287–95.
15. K. Yamaguchi: *Extraction 2018*, B. Davis, M. Moats, and S. Wang, eds., Springer, Cham, 2018, pp. 797–804. https://doi.org/10.1007/978-3-319-95022-8_63.
16. H.M. Henao, K. Yamaguchi, and S. Ueda: *Proceedings of Sohn International Symposium*, F. Kongoli, and R. Reddy, eds., TMS, Warrendale, 2006, vol. 1, pp. 723–29.
17. G. Roghani, J.C. Font, M. Hino, and K. Itagaki: *Mater. Trans. JIM*, 1996, vol. 37 (10), pp. 1574–79. https://doi.org/10.2320/matertrans1989.37.1574.
18. G. Roghani, M. Hino, and K. Itagaki: *Proceedings of 5th International Conference on Molten Slags, Fluxes and Salts*. Iron & Steel Society, Warrendale, 1997, pp. 693–703.
19. G. Roghani, M. Hino, and K. Itagaki: *Mater. Trans. JIM*, 1997, vol. 38 (8), pp. 707–13. https://doi.org/10.2320/matertrans1989.38.707.
20. G. Roghani, Y. Takeda, and K. Itagaki: *Metall. Mater. Trans. B*, 2000, vol. 31B (4), pp. 705–12. https://doi.org/10.1007/s11663-000-0109-9.
21. K. Avarmaa, L. Klemettinen, H. O'Brien, and P. Taskinen: *Miner. Eng.*, 2019, vol. 133, pp. 95–102. https://doi.org/10.1016/j.mineng.2019.01.006.
22. D. Sukhomlinov, L. Klemettinen, K. Avarmaa, H. O'Brien, P. Taskinen, and A. Jokilaakso: *Metall. Mater. Trans. B*, 2019, vol. 50B (4), pp. 1752–65. https://doi.org/10.1007/s11663-019-01576-2.
23. D. Sukhomlinov, K. Avarmaa, O. Virtanen, P. Taskinen, and A. Jokilaakso: *Miner. Process. Extr. Metall. Rev.*, 2019, pp. 1–7. https://doi.org/10.1080/08827508.2019.1634561.
24. T. Hidayat, J. Chen, P.C. Hayes, and E. Jak: *Metall. Mater. Trans. B*, 2019, vol. 50B (1), pp. 229–41. https://doi.org/10.1007/s11663-018-1448-8.
25. M. Chen, K. Avarmaa, L. Klemettinen, H. O'Brien, D. Sukhomlinov, J. Shi, P. Taskinen, and A. Jokilaakso: *Metall. Mater. Trans. B.*, 2020, vol. 51B (4), pp. 1495–1508. https://doi.org/10.1007/s11663-020-01861-5.
26. K. Avarmaa, H. O'Brien, H. Johto, and P. Taskinen: *J. Sustain. Metall.*, 2015, vol. 1 (3), pp. 216–28. https://doi.org/10.1007/s40831-015-0020-x.
27. K. Avarmaa, H. Johto, and P. Taskinen: *Metall. Mater. Trans. B*, 2016, vol. 47B (1), pp. 244–55. https://doi.org/10.1007/s11663-015-0498-4.
28. D. Shishin, T. Hidayat, J. Chen, P.C. Hayes, and E. Jak: *J. Sustain. Metall.*, 2019, vol. 5 (2), pp. 240–49. https://doi.org/10.1007/s40831-019-00218-w.
29. K. Avarmaa, H. O'Brien, and P. Taskinen: *Advances in Molten Slags, Fluxes, and Salts: Proceedings of the 10th International Conference on Molten Slags, Fluxes, and Salts 2016*, R. Reddy, P. Chaubal, P.C. Pistorius, and U. Pal, eds., TMS, Pittsburgh, Springer, Cham, 2016, pp. 193–202. https://doi.org/10.1007/978-3-319-48769-4_20.
30. K. Avarmaa, H. O'Brien, L. Klemettinen, and P. Taskinen: *J. Mater. Cycles Waste Manage.*, 2019, pp. 1-14. https://doi.org/10.1007/s10163-019-00955-w.
31. T. Hidayat, A.F. Mehrjardi, P.C. Hayes, and E. Jak: *Advances in Molten Slags, Fluxes, and Salts: Proceedings of the 10th International Conference on Molten Slags, Fluxes and Salts 2016*, R.G. Reddy, P. Chaubal, P.C. Pistorius, and U. Pal, eds., Springer, Cham, 2016, pp. 1207–20. https://doi.org/10.1007/978-3-319-48769-4_130.

32. E. Jak and P.C. Hayes: *Miner. Proc. Extr. Metall.*, 2008, vol. 117 (1), pp. 1–17. https://doi.org/10.1179/174328508X272344.
33. E. Jak and P.C. Hayes: *VII International Conference on Molten Slags Fluxes and Salts*, Capetown, SAIMM, Johannesburg, 2004, pp. 85–104.
34. A. Fallah-Mehrjardi, T. Hidayat, P.C. Hayes, and E. Jak: *Metall. Mater. Trans. B*, 2017, vol. 48B (6), pp. 3002–16. https://doi.org/10.1007/s11663-017-1073-y.
35. A. Fallah-Mehrjardi, T. Hidayat, P.C. Hayes, and E. Jak: *Metall. Mater. Trans. B*, 2017, vol. 48B (6), pp. 3017–3026. https://doi.org/10.1007/s11663-017-1076-8.
36. A. Fallah-Mehrjardi, T. Hidayat, P.C. Hayes, and E. Jak: *Metall. Mater. Trans. B*, 2018, vol. 49B (4), pp. 1732–39.
37. S. Sineva, A. Fallah-Mehrjardi, T. Hidayat, M. Shevchenko, D. Shishin, P.C. Hayes, and E. Jak: *J. Phase Equilib. Diffus.*, 2020, vol. 41, pp. 243–56. https://doi.org/10.1007/s11669-020-00810-8.
38. T. Hidayat, A. Fallah-Mehrjardi, P.C. Hayes, and E. Jak: *Metall. Mater. Trans. B*, 2020, vol. 51B (3), pp. 963–72. https://doi.org/10.1007/s11663-020-01807-x.
39. T. Hidayat, P.C. Hayes, and E. Jak: *J. Phase Equilib. Diffus.*, 2018, vol. 39 (2), pp. 138–51. https://doi.org/10.1007/s11669-018-0616-5.
40. A. Fallah-Mehrjardi, T. Hidayat, P. C. Hayes, and E. Jak: *Miner. Process. Extr. Metall.*, 2020, pp. 1–8. https://doi.org/10.1080/25726641.2020.1786658.
41. A. Fallah-Mehrjardi, T. Hidayat, P. C. Hayes, and E. Jak: *Miner. Process. Extr. Metall.*, 2020, pp. 1–8. https://doi.org/10.1080/25726641.2020.1786657.
42. M. Chen, Y. Sun, E. Balladares, C. Pizarro, and B. Zhao: *Calphad*, 2019, vol. 66, p. 101642. https://doi.org/10.1016/j.calphad.2019.101642.
43. Y. Sun, M. Chen, E. Balladares, C. Pizarro, L. Contreras, and B. Zhao: *Calphad*, 2020, vol. 69, p. 101751. https://doi.org/10.1016/j.calphad.2020.101751.
44. Y. Sun, M. Chen, E. Balladares, C. Pizarro, L. Contreras, and B. Zhao: *Calphad*, 2020, vol. 70, p. 101803. https://doi.org/10.1016/j.calphad.2020.101803.
45. I.V. Kojo, A. Jokilaakso, and P. Hanniala: *JOM*, 2000, vol. 52 (2), pp. 57–61.
46. I. V. Kojo and H. Storch: *Sohn International Symposium*, F. Kongoli and R. Reddy, eds., vol. 8, Warrendale (PA), TMS, 2006. pp. 225–38.
47. P. Taskinen: *Miner. Proc. Extr. Metall.*, 2011, vol. 120 (4), pp. 240–46. https://doi.org/10.1179/1743285511Y.0000000013.
48. M. Chen, K. Avarmaa, L. Klemettinen, J. Shi, P. Taskinen, and A. Jokilaakso: *Metall. Mater. Trans. B*, 2020, vol. 51B (4), pp. 1552–63. https://doi.org/10.1007/s11663-020-01874-0.
49. M. Chen, K. Avarmaa, L. Klemettinen, J. Shi, P. Taskinen, D. Lindberg, and A. Jokilaakso: *Metall. Mater. Trans. B*, 2020, vol. 51B (5), pp. 2107–18. https://doi.org/10.1007/s11663-020-01933-6.
50. J. Gisby, P. Taskinen, J. Pihlasalo, Z. Li, M. Tyrer, J. Pearce, K. Avarmaa, P. Björklund, H. Davies, M. Korpi, S. Martin, L. Pesonen, and J. Robinson: *Metall. Mater. Trans. B*, 2017, vol. 48B (1), pp. 91–98. https://doi.org/10.1007/s11663-016-0811-x.
51. R.H. Davies, A.T. Dinsdale, J.A. Gisby, J.A.J. Robinson, and A.M. Martin: *Calphad*, 2002, vol. 26 (2), pp. 229–71. https://doi.org/10.1016/S0364-5916(02)00036-6.
52. J.L. Pouchou and F. Pichoir: *Proceedings of the 11th International Congress on X-ray Optics and Microanalysis (ICXOM)*, London, ON, Canada, 4–8 August 1986, J.D. Brown and R.H. Packwood, eds., University of Western Ontario: London, ON, Canada, 1986, pp. 249–56.
53. J. Lin, Y. Liu, Y. Yang, and Z. Hu: *Solid Earth Sci.*, 2016, vol. 1 (1), pp. 5–27.
54. P. Sylvester: *Laser ablation-ICP-MS in the earth sciences: current practices and outstanding issues*. Mineralogical Association of Canada, Québec, Canada, 2008, vol. 40, pp. 1–348.
55. E. Van Achterberg, C. Ryan, S. Jackson, and W. Griffin: Laser Ablation ICP-MS in the Earth Science., Short Course Series #29, Mineralogical Association of Canada, St John, Newfoundland, 2001, pp. 239–43.
56. V. Malavergne, E. Charon, J. Jones, P. Cordier, K. Righter, D. Deldicque, and L. Hennet: *Earth Planet. Sci. Lett.*, 2016, vol. 434, pp. 197–207. https://doi.org/10.1016/j.epsl.2015.11.037.
57. A. Borisov and H. Palme: *Am. Mineral.*, 2000, vol. 85 (11–12), pp. 1665–73. https://doi.org/10.2138/am-2000-11-1209.
58. J.M. Toguri and N.H. Santander: *Metall. Mater. Trans. B*, 1972, vol. 3B (2), pp. 590–92. https://doi.org/10.1007/BF02642068.
59. N. Choi and W.D. Cho: *Miner. Metall. Proc.*, 1998, vol. 15 (3), pp. 23–29. https://doi.org/10.1007/BF03403220.
60. R. Altman and H.H. Kellogg: *Trans. Inst. Min. Metall. Sect. C*, 1972, vol. 81, pp. C163–75.
61. J.R. Taylor and J.H.E. Jeffes: *Trans. Inst. Min. Metall.*, 1975, vol. 84 (1), pp. C18–24.
62. D. Shishin, T. Hidayat, U. Sultana, M. Shevchenko, and E. Jak: *J. Sustain. Metall.*, 2019, vol. 6, pp. 68–77. https://doi.org/10.1007/s40831-019-00257-3.
63. K. Baba and K. Yamaguchi: *J. MMIJ*, 2013, vol. 129 (5), pp. 208–12. https://doi.org/10.2473/journalofmmij.129.208 (in Japanese).
64. M.A.H. Shuva, M.A. Rhamdhani, G.A. Brooks, S.H. Masood, and M.A. Reuter: *Metall. Mater. Trans. B*, 2017, vol. 48B (1), pp. 317–27. https://doi.org/10.1007/s11663-016-0839-y.
65. L. Klemettinen, K. Avarmaa, H. O'Brien, A. Jokilaakso, and P. Taskinen: *JOM*, 2020, vol. 72, pp. 2770–77. https://doi.org/10.1007/s11837-019-03960-4.
66. T. Murata and K. Yamaguchi: *J. Jpn. Inst. Met. Mater.*, 2020, vol. 84 (4), pp. 115–20. https://doi.org/10.2320/jinstmet.J2019046 (in Japanese).
67. C. Wiraseranee, T. Yoshikawa, T.H. Okabe, and K. Morita: *Mater. Trans.*, 2014, vol. 55 (7), pp. 1083–90. https://doi.org/10.2320/matertrans.M2014042.
68. J.J. Chen, C. Allen, P.C. Hayes, and E. Jak: *Advances in Molten Slags, Fluxes, and Salts: Proceedings of the 10th International Conference on Molten Slags, Fluxes and Salts 2016*, R.G. Reddy, P. Chaubal, P.C. Pistorius, and U. Pal, eds., Springer, Cham, 2016, pp. 961–70. https://doi.org/10.1007/978-3-319-48769-4_102.
69. K. Avarmaa: PhD thesis, *Thermodynamic Properties of WEEE-Based Minor Elements in Copper Smelting Processes*, Aalto University, 2019. https://aalto.finna.fi/Record/aaltodoc.123456789_39995.
70. M. Kashima, M. Eguchi, and A. Yazawa: *Trans. Jpn. Inst. Met.*, 1978, vol. 19 (3), pp. 152–58. https://doi.org/10.2320/matertrans1960.19.152.